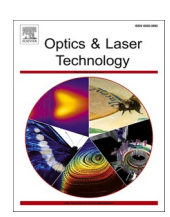
ELSEVIER

Contents lists available at ScienceDirect

Optics and Laser Technology

journal homepage: www.elsevier.com/locate/optlastec





Femtosecond optical Kerr gate with double gate pulses: Simulation and experiment

Wenjiang Tan^{*}, Jun Ma, Jinhai Si, Zhenqiang Huang, Xun Hou

Key Laboratory for Physical Electronics and Devices of the Ministry of Education, Shannxi Key Lab of Information Photonic Technique, School of Electronic Science and Engineering, Xi'an Jiaotong University, Xianning-xilu 28, Xi'an 710049, China

ARTICLE INFO

Keywords:
Optical Kerr gate
Femtosecond optical switch
Theoretical model
Optical Kerr materials

ABSTRACT

We demonstrated an improved optical Kerr gate with double gate pulses (D-OKG) to realize an ultrashort switching time even with a slow-response optical Kerr medium. A theoretical model of D-OKG was established and the dependence of the D-OKG performance on the relative intensity and the relative delay time of the two gate pulses was investigated. An integrated optimal condition was predicted. The D-OKG was experimentally built and optimized according to the simulation. The dependence of the D-OKG performance on the two gate pulses was confirmed. In our experiment, the achieved values for transmittance and switching time were 45 % and 150 fs, respectively. Compared to the conventional OKG, the D-OKG owns an integrated optimal performance in the femtosecond regime, and has the potential for a wide range of ultrafast optical switch applications.

1. Introduction

The femtosecond optical switch has been widely used in many fields, such as time-gated ballistic imaging [1-4], fuel spray dynamic diagnostics [5-7], time-resolved ultrafast fluorescence detection [8-11], Raman spectroscopy measurement [12] and three-dimensional object shape measurement [13,14]. As one of these femtosecond optical switches, the optical Kerr gate (OKG), based on the optical Kerr effect, is widely used to control the switching of light on an ultrafast timescale [15–16]. Generally, the OKG is composed of a pair of crossed polarizers around an isotropic Kerr medium. When the gate light is absent, the analyzer blocks the signal light introduced into the OKG, and the OKG closes. When the gate light is present, transient birefringence due to the optical Kerr effect is induced in the optical Kerr material, and the polarization direction of the linearly polarized signal light rotates. Parts of the signal light pass through the analyzer and the OKG opens. Compared to other nonlinear ultrafast optical switches, the phase-matching condition need not be satisfied with the OKG, which greatly improves the ease of use [17,18].

For the femtosecond optical switch, both a high transmittance and short switching time are necessary for a sufficient signal-to-noise ratio and high temporal resolution in ultrafast time-resolved measurements. However, in the femtosecond domain, most optical Kerr materials do not possess both a large optical nonlinearity or ultrafast response time [19].

For example, as two widely used optical Kerr materials, liquid carbon disulfide exhibits a very large optical nonlinearity but suffers a slow relaxation time, whereas solid fused quartz has an ultrafast response but suffers a low optical nonlinearity. Developments of new techniques are necessary to improve the OKG performance.

A double-stage OKG was proposed and applied to OKG ballistic photon imaging in order to reduce the switching time of CS_2 [20,21]. In the double-stage OKG, the signal light successively passes through the first and second OKGs when the transmittance windows of the two OKGs overlap. The double-stage OKG can limit light collection to an ultrashort time window if the two OKGs have an appropriate delay time, but it also unfortunately lowers the light transmittance. To obtain a higher signal intensity, an amplifying OKG was proposed with a simultaneous threedimensional shape measurement method [22,23]. In the amplifying OKG, a pyridine dye dissolved in acetonitrile was used as the optical Kerr material. A fundamental femtosecond pulse was first introduced using the frequency doubling of an LiB₃O₅ crystal and was then transformed into two perpendicularly polarized optical gating pulses with some optical delays by a birefringent β -BaB₂O₄ crystal. The first gating pulse was used to introduce an excited-state population and a simultaneous photoinduced birefringence in the dye solution, opening the OKG. The second gating pulse perpendicularly polarized to the first one was used to cancel the photoinduced anisotropy induced by the first gating pulse and close the OKG. The transmittance of the amplifying OKG was

E-mail address: tanwenjiang@mail.xjtu.edu.cn (W. Tan).

^{*} Corresponding author.

increased because the excited-state optical Kerr material was used. However, the restricted adjustable optical delay and light intensities and the long excited-state lifetime of the dye solution limit the switching time of the amplifying OKG to hundreds of femtoseconds. Recently, we also proposed an improved femtosecond optical Kerr gate with double gate pulses (D-OKG) using common carbon disulfide (CS₂) as the optical Kerr material. Our research indicated that this D-OKG retains a high transmittance comparable to that of a conventional OKG using CS₂, and simultaneously has an ultrashort switching time comparable to that of a conventional OKG using fused silica [24]. However, our previous experimental study did not fully reveal the comprehensive performance of the D-OKG on the experimental parameters to guide its actual optimization process.

In this study, we further developed the theoretical model of the D-OKG and numerically investigated the dependence of the D-OKG performance on the key experimental parameters. By evaluating the signal transmittance, the switching time and the contrast of the D-OKG, a theoretical D-OKG optimization strategy was suggested. We also experimentally studied the dependence of the D-OKG performance on some different conditions, which agreed well with the theoretical prediction. The results provide a valid optimization strategy of the D-OKG for its practical applications.

2. Theoretical model

For the Kerr effect, the polarization rotation of the signal light is determined by Δn , the difference between the induced refractive indices parallel and perpendicular to the optical electric field of the gate light. Assuming the gate pulse obeys a Gaussian distribution in time, Δn can be given by [25]

$$\Delta n^e = \frac{1}{2} n_2^e E_0^2 exp \left[-\left(\frac{t}{\tau_1}\right)^2 \right] \tag{1}$$

$$\Delta n^{o} = \frac{\sqrt{\pi}}{4} n_{2}^{o} E_{0}^{2} \frac{\tau_{1}}{\tau_{o}} exp \left[-\frac{t}{\tau_{o}} + \left(\frac{\tau_{1}}{2\tau_{o}} \right)^{2} \right]$$

$$\times \operatorname{erfc} \left[-\frac{t}{\tau_{1}} + \frac{\tau_{1}}{2\tau_{0}} \right], \tag{2}$$

where Δn^e represents the ultrafast response of the Kerr medium, such as instantaneous electronic cloud distortion, to the electric field, and Δn^o represents the relatively slow response of the Kerr medium, such as molecular orientation. E_0 represents the peak amplitude of the gate pulse. τ_1 represents the time constant (half width at 1/e of intensity) of the gate pulse, which relates to the commonly used pulse width at half maximum as $2\tau_1(\ln 2)^{1/2}$. n_2^e and n_2^o represent the ultrafast and relatively slow parts of the nonlinear optical refractive indices. τ_o is the relaxation time of the molecular reorientation and is an important reason for the low temporal resolution. In the D-OKG, the transient birefringence is induced by two perpendicularly polarized gate pulses, which have the same frequency and propagation direction. Based on the tensor properties of the polarizability and the spatial symmetry of isotropic media, Δn can be given by:

$$\Delta n = \Delta n_1 \left(I_{g1}, t \right) - \Delta n_2 \left(I_{g2}, t + \tau_R \right) \tag{3}$$

where τ_R is the relative delay time between the two gate pulses and I_{g1} and I_{g2} are the peak light intensities of the two gate pulses. When a signal pulse travels through the Kerr medium of thickness L, the phase shift is

$$\Delta\varphi(t) = \frac{2\pi}{\lambda} \Delta n(t) \cdot L \tag{4}$$

Here, for simplicity, the signal pulse and gate pulses have the same frequency (same group velocity) and direction of propagation. The transmittance of the OKG is defined as the intensity ratio of the parts

through the analyzer and all signal light induced to the optical Kerr medium, and can be given by [2]

$$T = \frac{\int_{-\infty}^{\infty} I_s(t - \Delta t) \cdot \sin^2\left(\frac{\Delta \varphi(t)}{2}\right) \sin^2(2\Phi) dt}{\int_{-\infty}^{\infty} I_s(t) dt}$$
 (5)

where I_s is the intensity of the signal pulse induced to the optical Kerr medium, and Φ and Δt denote the angle of polarization and the delay time between the signal pulse and gate pulse, respectively.

3. Experimental setup

Fig. 1 shows a schematic of the D-OKG in our experiment. A Ti: sapphire laser system, emitting 50-fs, 4-mJ and 800-nm linearly polarized laser pulses at a repetition rate of 1 kHz, was used in our experiments. A 50/50 beam splitter BS1 is used to split the laser beam into two parts. The transmitted part is used as the signal pulse, while the reflected part first passes through an optical delay line (ODL1) and then splits into two gate pulses. The two gate pulses are adjusted to the same direction of propagation by beam splitter BS3, and then introduced to the OKG. The OKG consists of a pair of crossed Glan-Taylor polarizers and an optical Kerr medium between them. The angle between the propagation direction of the gate pulses and the signal pulse is about 8.5°.

In the experiment, ODL1 was used to adjust the temporal overlap between the gate pulses and the signal pulse in the optical Kerr medium. Two adjustable neutral optical attenuators (AA2, AA3) and an optical delay line (ODL2) were used to separately adjust the intensity of the double gate pulses and the relative delay time τ_R . Two half-wave plates (HWP1, HWP2) were separately inserted in the gate pulse paths to ensure their polarizations were perpendicular to each other. In order to obtain the maximum transmission efficiency, the polarizations of the two gate pulses were respectively rotated by $\pi/4$ and $-\pi/4$ with respect to the polarizer in the experiment. The extinction ratio of the polarizers used here was greater than 105. CS2 filled in a glass cuvette with a geometric path length of 5 mm was used as the main optical Kerr medium. The signal pulse and the gate pulses were all weakly focused to a spot of hundreds of micrometers and overlapped in the optical Kerr medium, and the gate pulses after the Kerr medium were blocked. The energies of the first gate pulse and the signal pulse were set to 16 and 1 μJ/pulse, respectively. The light spot diameters of the gate pulses and the signal pulse at the optical Kerr material surface were measured to be about 280 and 150 µm, respectively. When the OKG was opened by the gate pulses, the OKG signals were detected by a biased silicon photodetector (ET-2020, Electro-Optics Technology Inc., USA). The rise and fall time of the detector are both less than 1.5 ns.

4. Results and discussion

Compared to traditional OKGs, the D-OKG has two gate light beams passing through the optical Kerr medium. The first gate light is used to induce transient birefringence, while the second is used to suppress it. The D-OKG signals at different I_g : I_{g2} and τ_R were simulated to determine how the D-OKG changes with the second gate light.

The simulation parameters were as follows: $E_{0g1}=2.2\times10^8$ V/m, $\Phi=\pi/4$, $\lambda=800$ nm, $\tau_1=100$ fs, L=5 mm, $\tau_0=2$ ps, $n_2{}^o=2.0\times10^{-20}$ m $^2/V^2$ and $n_2{}^e=2.1\times10^{-21}$ m $^2/V^2$ [2]. A wider laser pulse was used in the simulation because of the evident influence of the dispersion and some geometric parameters of the light, such as the spatial distribution, difference in propagation direction [26] and convergence of light in the experiment.

Firstly, the dependence of D-OKG on τ_R is investigated. We set $I_{g1}:I_{g2}=1:0.7$ and τ_R varying from 100 to 500 fs to some typical value and compared the results by adjusting τ_R . Fig. 2(a) presents the simulated transmittance of the D-OKG when $I_{g1}:I_{g2}=1:0.7$ and τ_R varies from 100 to 500 fs. From Eq. (3), if τ_R is smaller than 300 fs, the peak

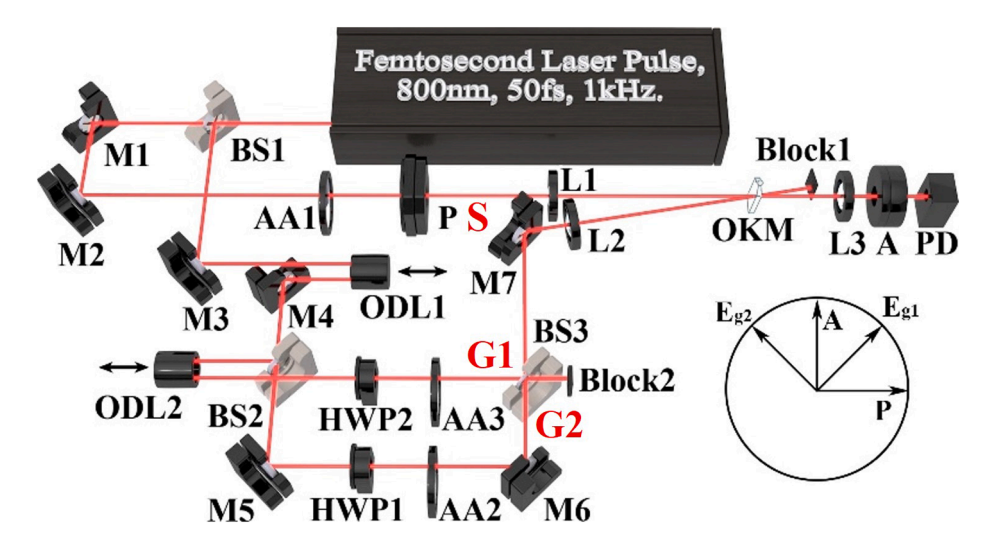


Fig. 1. Schematic of the D-OKG and the polarization of the pump beams. M: mirror, L: lens, BS: beam splitter, ODL: optical delay line, HWP: half-wave plate, AA: adjustable attenuator, P: polarizer, A: analyzer, OKM: optical Kerr medium, PD: photodiode, S: signal beam, G1 and G2: gate beam 1 and gate beam 2.

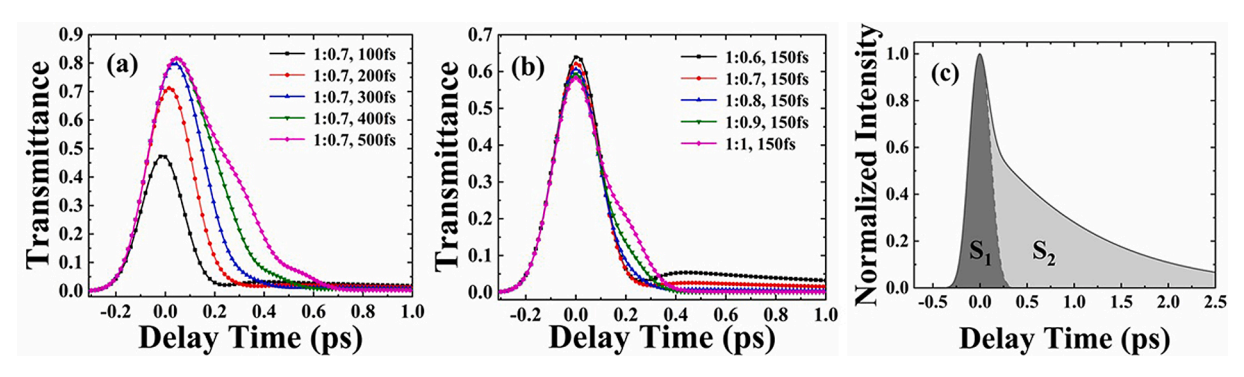


Fig. 2. (a) Simulated transmittance of D-OKGs when $I_{g1}:I_{g2}=1:0.7$ at different τ_R . (b) Simulated transmittance of D-OKGs when $\tau_R=150$ fs at different $I_{g1}:I_{g2}$. (c) Schematic of the definition of contrast. S_1 is the symmetrical area; S_2 is the asymmetrical area. The zero-delay time is fixed to the peak transmittance.

transmittance is influenced by the second gate pulse, and decreases when τ_R decreases. When τ_R is larger than 300 fs, the peak transmittance is only determined by Δn_1 and remains unchanged with the second gate pulse.

Secondly, the dependence of D-OKG on I_{g1} : I_{g2} is investigated. We set τ_R to some typical value and compared the results by adjusting I_{g2} . Fig. 2 (b) shows the simulated transmittance of the D-OKG when $\tau_R=150$ fs and I_{g1} : I_{g2} varies from 1:0.6 to 1:1. It shows that the transmittance at different I_{g2} is almost the same at negative delay times, while is different at positive delay times. When I_{g2} increases, the peak transmittance decreases, and the switching time decreases. The excessive effect of the second gate pulse sometimes leads to side lobes. This can be explained using the theory of molecular reorientation. Molecular reorientation is induced by the first gate pulse, and cancelled by the second gate pulse. If the second gate pulse is too strong, new molecules reorientation will be produced.

The simulation shows that D-OKG's performance is influenced by $I_{\rm g2}$ and $\tau_{\rm R}$. So we tried to find the optimal performance and predict the optimal conditions of the D-OKG using multiple simulations. We used the peak transmittance ($T_{\rm p}$: maximum transmittance at different delay times), the switching time ($t_{\rm s}$: full width at half maximum (FWHM)) and the contrast (C) to describe the overall performance of the D-OKGs. The peak transmittance and the switching time are usually used to describe the intensity and temporal resolution of an optical switch. In addition, we used the contrast to describe the symmetry of the D-OKG. As shown in Fig. 2(c), the contrast is defined as the ratio of the symmetric part to the whole, and the contrast of the gate is $S_1/(S_1 + S_2)$. A symmetrical

switch usually performs better in applications because of weaker side lobes or less signal leakage than an asymmetrical switch. From Fig. 2(b), the gates have an almost equal switching time but their performance is different because of different contrast.

We tried to determine how the three parameters varied with $I_{\rm g2}$ and τ_R through simulation. Fig. 3 illustrates the relationship between peak transmittance, switching time (FWHM), contrast and I_{g2} : I_{g1} and τ_R . The D-OKG signals change according to some rules. From Fig. 3(a), with the decrease in I_{g2} , the peak transmittance increases; when $I_{g2} = 0$, the switch is a traditional OKG and the peak transmittance reaches a maximum. With the increase in τ_R , the peak transmittance increases and reaches a maximum when τ_R is larger than about 300 fs because of the weak intensity of the second gate pulse at zero delay time. From Fig. 3 (b), when τ_R increases, the switching time first decreases and then increases. When τ_R is less than about 300 fs, the switching time first decreases and then increases with I_{g2} . When τ_R is too short, not only the relaxation process of the slow response is influenced by the second gate pulse, but also the process of transient birefringence induction, so the switching time is larger than when τ_R is slightly larger. If I_{g2} is too large, the effect on the second gate pulse also becomes excessive, increasing the switching time. From Fig. 3(c), the contrast first increases and then decreases with the increase in I_{g2} or τ_R . The contrast is often lower if the switching time is larger at the same conditions. Side lobes or other kinds of signal leakages also lead to a decrease in contrast.

D-OKG's optimal conditions require a balance among the three parameters. For example, to reach the minimum switching time, the transmittance must be sacrificed. We use the weighted switching time to

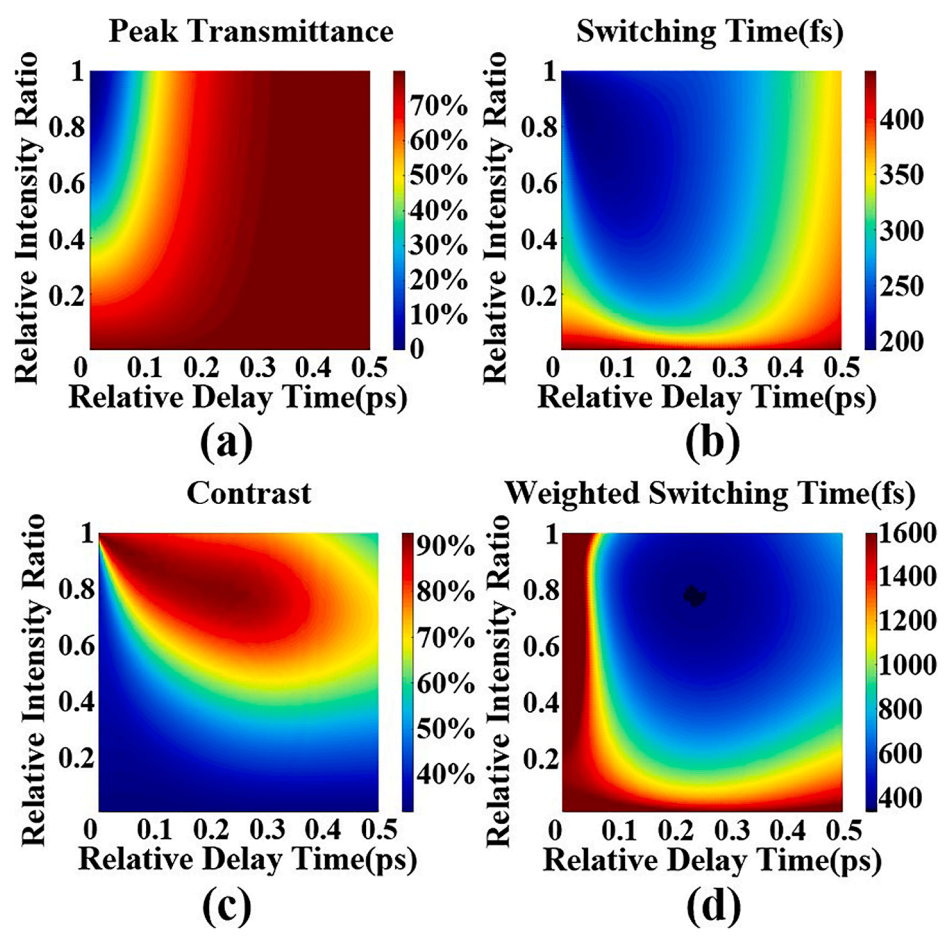


Fig. 3. (a) Peak transmittance, (b) switching time, (c) contrast and (d) weighted switching time at different relative intensity ratios I_{g2} : I_{g1} and relative delay times τ_R . S_1 and S_2 are the areas in $[-6\tau_1, 24\tau_1]$. The weighted switching time is $t_s/(T_p*C)$.

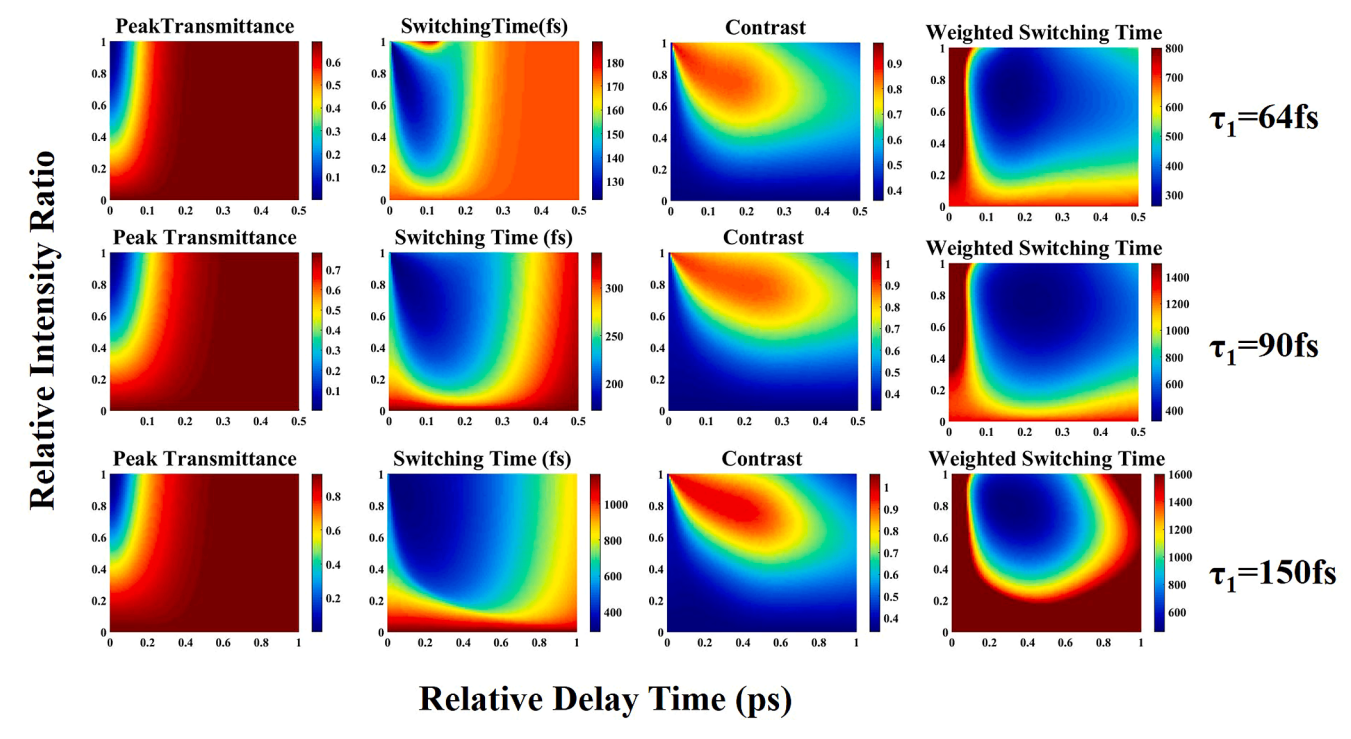


Fig. 4. Simulation of the dependence of the D-OKG performance on the experimental parameters at different input laser pulse durations.

describe the overall performance of a switch based on the three parameters. The weighted switching time is determined by the requirement of the application. To achieve a higher transmittance, lower switching time and higher contrast, the weighted switching time could be defined as $t_{\rm s}/(T_{\rm p}^*C)$ or $t_{\rm s}/(2^*T_{\rm p}^{-2}*C)$, etc. Fig. 3(d) shows the weighted switching time $t_{\rm s}/(T_{\rm p}^*C)$ at different $I_{\rm g2}$: $I_{\rm g1}$ and τ_R values. From Fig. 3(d), the simulated optimal conditions are $I_{\rm g2}$: $I_{\rm g1} = 0.77$ and $\tau_R = 245$ fs, and the D-OKG has the shortest weighted switching time and optimal performance.

It should be noted that the simulation shown the $\tau_1=100$ fs was selected as an example for the simulation to reveal the dependence of the D-OKG performance on the experimental parameters in Fig. 3. To find out the influence of using other pulse durations on the simulation, $\tau_1=64$ fs, 90 fs, and 150 fs were also used to perform the simulation, respectively. As the results shown in Fig. 4, for different input laser pulse durations, the dependences of the D-OKG performance on the experimental parameters shows similar trends. Of course, the relative intensity and the relative delay time of the two gate pulses were different at a fixed transmittance or switching time for different input laser pulse duration. For example, the optimal conditions for the shortest weighted switching time changed when $\tau_1=90$ fs, the simulated optimal conditions are $I_{\rm g2}:I_{\rm g1}=0.77$ and $\tau_R=230$ fs.

. To ensure the validity of above simulations, three D-OKG signals were then measured and compared with the simulations with $I_{g1}:I_{g2}=$ 1:0, 1:0.7, and 1:0.8 at $\tau_R = 180$ fs. The results were shown in Fig. 5. From Fig. 5, we can see that the simulation results agree well with the experimental D-OKG signals when $I_{g1}:I_{g2}=1:0.7$, and 1:0.8. Although the intensities and corresponding time delay of the two side lobes in simulations were different from the experimental results, the simulation and the experimental results indeed show the similar dependence on the time delay, which indicates the validity of our simulations shown above. Of course, we can also see that there is some difference between the simulated and the experimental result when I_{g1} : $I_{g2}=1$:0, namely, the simulated and the experimental OKG signals were compared. We infer that all the differences shown in Fig. 5 can be attribute to the noncollinear experimental arrangements and the collinear simulation model. For example, the temporal resolution in femtosecond pump-probe experiment will increase with increasing the intersection angle between the pump and the probe beams [26]. To eliminate the deviations between the simulations and the experimental results, a more precise noncollinear D-OKG simulation model is developing in our group.

Finally, according to the simulation results, a series of D-OKG and OKG signals were measured experimentally. As the gate pulses duration

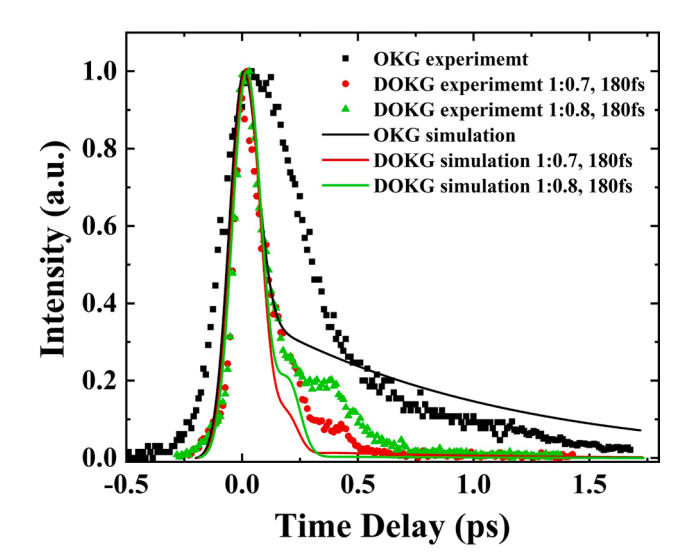


Fig. 5. Comparisons of the D-OKG signals and the simulations when I_{g1} : I_{g2} = 1:0, 1:0.7, and 1:0.8 at τ_R = 180 fs.

after lens 2 was measured to be approximately 105 fs using a homebuilt frequency-resolved optical gating setup, which relates to the time constant (half width at 1/e of intensity) of the gate pulse $\tau_1=64$ fs. We adjusted $I_{\rm g2}$ and $\tau_{\rm R}$ and measured the D-OKG signals around the conditions like $I_{\rm g2}$: $I_{\rm g1}=0.74$ and $\tau_{\rm R}=155$ fs according to Fig. 4. We also adjusted $I_{\rm g2}$ to zero and measured the conventional OKG signals with the Kerr medium CS2 and fused silica at the same experimental conditions. Fig. 6 shows the comparison of the switching characteristics of the D-OKG at different conditions and OKG with CS2 and OKG with fused silica. It shows the intensity, which has been normalized by their peak transmittance, and the transmittance at different delay times. The peak transmittance, switching time, contrast, and weighted switching time of the gates in the experiment are listed in Table 1.

By comparison of the normalized intensity, the switching time of the D-OKG is apparently less than that of the OKG with CS₂ (~400 fs) and very close to the OKG with fused silica (~130 fs). The contrast of the D-OKGs is apparently higher than that of the OKG with CS₂. By comparison of the transmittance, the peak transmittance of the D-OKGs is a bit lower than that of the OKG with CS_2 (~70 %), and apparently higher than that of the OKG with fused silica (~4 %). Fig. 6(a) shows the comparison of the D-OKGs at $\tau_R = 180$ fs and I_{g1} : I_{g2} from 1:0.6 to 1:0.9. From Fig. 4(a) and Table 1, both the switching time and peak transmittance decrease, and the contrast first increases and then decreases with the increase of $I_{\rm g2}$. Clear side lobes appear when $I_{\rm g1}$: $I_{\rm g2}$ is 1:0.8 or 1:0.9. Fig. 6(b) shows the comparison of the D-OKGs at $I_{\rm g1}$: $I_{\rm g2}=1:0.7$ and $\tau_{\rm R}$ from 150 to 240 fs. From Fig. 6(b) and Table 1, the peak transmittance increases with τ_R ; the switching time first decreases and then increases, the contrast first increases and then decreases when τ_R increases. The intensity of the side lobes also changes with τ_R and reaches a minimum when $\tau_R = 180$ fs. The weighted switching time first decreases and then increases with the increase of I_{g2} or τ_R , reaching a minimum when $\tau_R = 180$ fs and $I_{g1}:I_{g2} =$ 1:0.7. From Table 1, the weighted switching time of D-OKGs are apparently shorter than traditional OKGs. The change of D-OKG with the second gate pulse in the experiment are consistent with that in the simulation. The optimal condition in the experiment is I_{g1} : $I_{g2} = 1:0.7$ and $\tau_R = 180$ fs. At these conditions, the switching time is about 150 fs, the peak transmittance is about 45% and the side lobe is well-restricted.

5. Conclusions

In summary, we proposed an improved optical Kerr gate with a double gate pulse to realize an ultrashort switching time even with a slow-response optical Kerr medium, of which the intensities and relative optical delays of the two gate pulses were separately adjustable. We established the theoretical model of D-OKG. Based on simulations, we determined how the peak transmittance, switching time and contrast of the D-OKG changed with the second gate pulse. The results indicated that, when the relative intensity increases or the relative delay time decreased, the transmittance decreases, and when the relative intensity or the relative delay time increased, the switching time decreases first and then increases, and the contrast increases first and then decreases. We also proposed a strategy to predict the optimal conditions of D-OKG using the weighted switching time. By adjusting the intensity of the second gate pulse and the relative delay time, a high transmittance, short switching time and high contrast were achieved. In this experiment, the DOKG has the optimal performance when the intensity ratio of the two gate pulses is 1:0.7 and the relative delay time is 180 fs. At these conditions, the switching time was 150 fs, the peak transmittance was 45%, and the side lobes were well-restricted. As the intensity and the relative delay time are easy to adjust, the performance of the D-OKG can be conveniently changed according to different applications. Compared to other techniques, the D-OKG is also adjustable and more convenient. The D-OKG has the potential for a wide range of applications and performs better than other traditional optical switches.

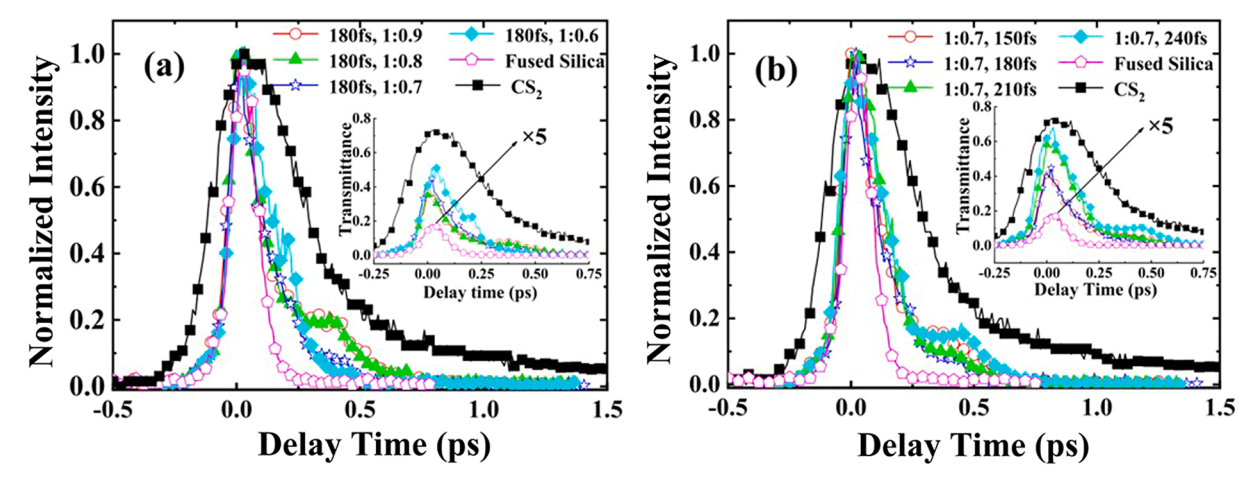


Fig. 6. Normalized intensity and transmittance of D-OKGs at different (a) I_{g1} : I_{g2} and (b) τ_R values and the OKG with the Kerr medium CS₂ and fused silica at different delay times. The zero-delay time has been set to the peak transmittance.

Table 1
D-OKG's performance in experiment and its comparison to traditional OKG.

| | Conditions | Peak transmittance | Switching time | Contrast | Weighted switching time |
|--------------------------|--------------|--------------------|----------------|----------|-------------------------|
| D-OKG (CS ₂) | 1:0.6,180 fs | 51.2% | 174.3 fs | 65.4% | 520.4 fs |
| | 1:0.7,180 fs | 44.8% | 149.7 fs | 73.9% | 452.0 fs |
| | 1:0.8,180 fs | 35.5% | 151.8 fs | 61.3% | 698.4 fs |
| | 1:0.9,180 fs | 36.6% | 139.2 fs | 60.7% | 626.1 fs |
| | 1:0.7,150 fs | 40.7% | 165.6 fs | 63.0% | 645.7 fs |
| | 1:0.7,180 fs | 44.8% | 149.7 fs | 73.9% | 452.0 fs |
| | 1:0.7,210 fs | 58.2% | 189.7 fs | 62.0% | 525.7 fs |
| | 1:0.7,240 fs | 68.0% | 208.2 fs | 56.9% | 537.8 fs |
| OKG (CS ₂) | | 73.0% | 412.9 fs | 52.7% | 1073.3 fs |
| OKG (fused silica) | | 4.2% | 129.3 fs | 90.6% | 3398.0 fs |

Declaration of Competing Interest

The authors declare that they have no known competing financial interests or personal relationships that could have appeared to influence the work reported in this paper.

Acknowledgements

This work is supported by the National Natural Science Foundation of China (62027822, 61690221, 62175197), the National Key Research and Development Program of China (2019YFA0706402), the Natural Science Basic Research Program of Shaanxi Province of China (2018JM6012), and the Fundamental Research Funds for the Central Universities (xzy012019039).

References

- [1] L. Wang, P.P. Ho, C. Liu, G. Zhang, R.R. Alfano, Ballistic 2-D imaging through scattering walls using an ultrafast optical Kerr gate, Science 253 (5021) (1991) 769–771
- [2] F. Mathieu, M.A. Reddemann, J. Palmer, R. Kneer, Time-gated ballistic imaging using a large aperture switching beam, Opt. Express 22 (6) (2014) 7058, https://doi.org/10.1364/OE.22.007058.
- [3] L. Wang, P.P. Ho, X. Liang, H. Dai, R.R. Alfano, Kerr-Fourier imaging of hidden objects in thick turbid media, Opt. Lett. 18 (3) (1993) 241, https://doi.org/ 10.1364/OL.18.000241.
- [4] J.B. Schmidt, Z.D. Schaefer, T.R. Meyer, S. Roy, S.A. Danczyk, J.R. Gord, Ultrafast time-gated ballistic-photon imaging and shadowgraphy in optically dense rocket sprays, Appl. Opt. 48 (4) (2009) B137, https://doi.org/10.1364/AO.48.00B137.
- [5] D. Sedarsky, M. Rahm, M. Linne, Visualization of acceleration in multiphase fluid interactions, Opt. Lett. 41 (7) (2016) 1404, https://doi.org/10.1364/ 01.41.001404
- [6] Z. Falgout, M. Rahm, D. Sedarsky, M. Linne, Gas/fuel jet interfaces under high pressures and temperatures, Fuel 168 (2016) 14–21.

- [7] M. Rahm, M. Paciaroni, Z. Wang, D. Sedarsky, M. Linne, Evaluation of optical arrangements for ballistic imaging in sprays, Opt. Express 23 (17) (2015) 22444, https://doi.org/10.1364/OE.23.022444.
- [8] J.C. Blake, J. Nieto-Pescador, Z. Li, L. Gundlach, Ultraviolet femtosecond Kerrgated wide-field fluorescence microscopy, Opt. Lett. 41 (11) (2016) 2462, https://doi.org/10.1364/OL.41.00246210.1364/OL.41.002462.v001.
- [9] K. Appavoo, M.Y. Sfeir, Enhanced broadband ultrafast detection of ultraviolet emission using optical Kerr gating, Rev. Sci. Instrum. 85 (5) (2014) 055114, https://doi.org/10.1063/1.4873475
- [10] L. Gundlach, P. Piotrowiak, Femtosecond Kerr-gated wide-field fluorescence microscopy, Opt. Lett. 33 (9) (2008) 992, https://doi.org/10.1364/OL.33.000992.
- [11] T. Fujino, T. Fujima, T. Tahara, Picosecond time-resolved imaging by nonscanning fluorescence Kerr gate microscope, Appl. Phys. Lett. 87 (13) (2005) 131105, https://doi.org/10.1063/1.2067694.
- [12] F. Knorr, Z.J. Smith, S. Wachsmann-Hogiu, Development of a time-gated system for Raman spectroscopy of biological samples, Opt. Express 18 (19) (2010) 20049, https://doi.org/10.1364/OE.18.020049.
- [13] K. Minoshima, H. Matsumoto, Z. Zhang, T. Yagi, Simultaneous 3-D imaging ising chirped ultrashort optical pulses, Jpn. J. Appl. Phys. 33 (1994) L1348–L1351.
- [14] K. Minoshima, T. Yasui, E. Abraham, H. Matsumoto, G. Jonusauskas, C. Rulliere, Three-dimensional imaging using a femtosecond amplifying optical Kerr gate, Opt. Eng. 38 (1998) 1758–1762.
- [15] M.A. Duguay, J.W. Hansen, An ultrafast light gate, Appl. Phys. Lett. 15 (6) (1969) 192–194.
- [16] P.D. Maker, R.W. Terhune, C.M. Savage, Intensity-dependent changes in the refractive index of liquids. Phys. Rev. Lett. 12 (18) (1964) 507–509.
- [17] C. Calba, L. Méès, C. Rozé, T. Girasole, Ultrashort pulse propagation through a strongly scattering medium: simulation and experiments, J. Opt. Soc. Am. A 25 (7) (2008) 1541, https://doi.org/10.1364/JOSAA.25.001541.
- [18] M. Bashkansky, C.L. Adler, J. Reintjes, Coherently amplified Raman polarization gate for imaging through scattering media, Opt. Lett. 19 (5) (1994) 350, https://doi.org/10.1364/OL.19.000350.
- [19] P.P. Ho, R.R. Alfano, Optical Kerr effect in liquids, Phys. Rev. A 20 (5) (1979) 2170–2187.
- [20] L.M. Wang, P.P. Ho, R.R. Alfano, Double-stage picosecond Kerr gate for ballistic time-gated optical imaging in turbid media, Appl. Opt. 32 (4) (1993) 535, https://doi.org/10.1364/AO.32.000535.
- [21] D. Sedarsky, S. Idlahcen, K. Lounnaci, J.B. Blaisot, C. Rozé, Diesel spray velocity and break-up characterization with dense spray imaging, in: Proceedings of 12th

- Triennial International Conference on Liquid Atomization and Spray Systems,
- [22] T. Yasui, K. Minoshima, E. Abraham, H. Matsumoto, Microscopic time-resolved two-dimensional imaging with a femtosecond amplifying optical Kerr gate, Appl. Opt. 41 (24) (2002) 5191, https://doi.org/10.1364/AO.41.005191.
- [23] G. Jonusauskas, J. Oberlé, E. Abraham, C. Rullière, "Fast" amplifying optical Kerr gate using stimulated emission of organic non-linear dyes, Opt. Commun. 137 (1-3) (1997) 199–206.
- [24] W. Tan, J. Ma, Y. Zheng, J. Tong, Femtosecond optical Kerr gate with double gate pulses, IEEE Photon. Technol. Lett. 30 (3) (2018) 266–269.

 [25] K. Sala, M.C. Richardson, Optical Kerr effect induced by ultrashort laser pulses,
- Phys. Rev. A 12 (3) (1975) 1036–1047.
- [26] M. Ziolek, R. Naskrecki, M. Lorenc, J. Karolczak, J. Kubicki, A. Maciejewski, The influence of the excitation geometry on the temporal resolution in femtosecond pump-probe experiments, Opt. Commun. 197 (4-6) (2001) 467–473.